*Computers and Concrete, Vol. 3, No. 2/3 (2006) 123-144*
DOI: http://dx.doi.org/10.12989/cac.2006.3.2/3.123 

# Nonlinear finite element analysis of reinforced concrete corbels at both deterministic and probabilistic levels

Alfred Strauss†

*Department of Civil Engineering + Natural Hazards, Institute for Structural Engineering, University of Natural Resources and Applied Life Sciences, Vienna, Austria*

Andrea Mordini‡

*Department of Civil Engineering, University of Parma, Parma, Italy*

Konrad Bergmeister

*Department of Civil Engineering + Natural Hazards, Institute for Structural Engineering, University of Natural Resources and Applied Life Sciences, Vienna, Austria*

*(Received November 28, 2005, Accepted May 23, 2006)*

**Abstract.** Reinforced concrete corbels are structural elements widely used in practical engineering. The complex response of these elements is described in design codes in a simplified manner. These formulations are not sufficient to show the real behavior, which, however, is an essential prerequisite for the manufacturing of numerous elements. Therefore, a deterministic and probabilistic study has been performed, which is described in this contribution. Real complex structures have been modeled by means of the finite element method supported primarily by experimental works. The main objective of this study was the detection of uncertainties effects and safety margins not captured by traditional codes. This aim could be fulfilled by statistical considerations applied to the investigated structures. The probabilistic study is based on advanced Monte Carlo simulation techniques and sophisticated nonlinear finite element formulations.

**Keywords:** corbels; reinforced concrete; experimental program; reliability; probabilistic study; safety margins; high developed Monte Carlo simulation; nonlinear finite element concept; 2D and 3D models.

## 1. Introduction

Corbels are widely used in precast concrete structures due to the main advantages of better concrete quality, improved production speed, and lower construction costs. During the past century, many different theories (Holnicki-Szulc & Gierlinski 1997, Ali & White 2001) have been proposed to describe corbel behavior, and several experimental programs have been carried out to investigate

† Visiting Student, Corresponding Author, E-mail: alfred.strauss@boku.ac.at
‡ Civil Engineer, PhD., http://www.andreamordini.com

these structures from the practical point of view.

This paper aims at describing the behavior and the load carrying capacity of reinforced concrete (RC) corbels as closely as possible to the reality shown by experimental test series. The numerical and experimental results rely on extensive studies performed at the University of Natural Resources and Applied Life Sciences, Vienna (Mordini and Strauss 2005).

The aim in the first step of the research program was to capture the behavior of corbels taken from experimental programs (Kriz, *et al.* 1965) by using highly developed nonlinear finite element codes. While there are several nonlinear codes, only some of them are capabable of capturing the complex mechanisms in concrete structures, like crack initiation, softening, and hardening.

The study results in the selection of a two-dimensional (2D) RC-oriented Finite Element (FE) code, named ATENA, which delivers a very good agreement with the experimental data during the testing processes up to the failure. Since the complex material laws demand numerous input properties to be fitted, evaluation of the corbels is initially performed in a deterministic way. During the deterministic calculation, the development of strain/stress fields, crack initiation, crack propagation, the crack pattern and the post-peak behavior of the corbels, as well as the load capacity compared to design code formulations (CEB 1993) were of interest. Several different specimens, including the Steel Fiber Reinforced Concrete (SFRC) type, were simulated in order to fit and verify the material parameter and the overall structural behavior.

Based on the knowledge of the variability of material properties, the second research period focused on the aspect of randomness: probabilistic analysis. The aim was to verify the existing safety index of design codes and to evaluate the sensitivity of the elements responsible for the corbels' load capacity. ATENA, the software used for this purpose, is an integral part of the extended tool SARA (Structural Analysis and Reliability Assessment) for the probabilistic treatment of the problem under investigation (Pukl, *et al.* 2003). The second part of the system is the probabilistic tool FREET, which makes efficient use of a stratified Monte Carlo technique called Latin Hypercube Sampling (LHS) (Novák, *et al.* 2003). Its advantage is that, compared to the classical Monte Carlo method, it only needs a small number of samples to get good estimates of basic statistics. This feature is essential for the time consuming nonlinear FE analysis. Therefore, the uncertainties related to the materials could be simulated efficiently by a randomization process. For each of the corbels, 50 random samples, described by probability distributions, were used to evaluate the load capacity and to find out the dominating random variables responsible for the fracture process propagation (sensitivity analysis). In a further step, the probabilistic analysis served for the probabilistic assessment of the safety margins provided by Eurocodes.

Based on the promising outcomes of the study in the 2D analysis, the corbels were also investigated taking into account three-dimensional (3D) effects – the codes used (ATENA, SARA, FREET) were recently extended to 3D. For these considerations, different constitutive models of concrete were used.

## 2. The structural and reliability analysis backgrounds

Concrete structures exhibit complex behavior even for low load levels (Menétrey, *et al.* 1995). Nonlinear compressive stress-strain relation, tensile cracking, post-cracking softening and interaction effects between concrete and reinforcing bars (Cervenka 1985) are the main sources of a highly nonlinear and complicated response. Therefore, sophisticated numerical tools are necessary to capture the real structural behavior. ATENA, the code that was used, is an effective and reliable tool for nonlinear analysis of RC structures that has been developed by Cervenka Consulting. It has been validated by many different applications and examples (Cervenka 2000, 2002).

Advanced material models based on hyperelasticity or fracture-plasticity (Cervenka, *et al.* 1998) approaches are implemented in ATENA. Cracking phenomena are modeled by the smeared crack approach (Cervenka 1985), both fixed and rotating cracks can be considered. The code allows for modeling the reinforcements as smeared and discrete elements, and bond effects can be captured by using several bond-slip laws. In addition, the constitutive models are fully customizable and allow for modifying the material parameters or introducing user-defined laws. Monitoring points in the model serve to extract interesting outcomes in particular locations. Several advanced solving techniques are implemented, including Newton-Raphson, modified Newton-Raphson, Arc Length, and line search (Crisfield 1983). These properties and characteristics are used to formulate the numerical models of the corbels.

The behavior of concrete structures is mainly related to material and geometric properties. The randomness (material, geometry, boundary conditions etc.) inherent in structures is one of the main problems in practice and, therefore, also in numerical modeling. Probabilistic approaches in combination with nonlinear numerical modeling can reduce this weakness and allow a more realistic evaluation of practical design and design techniques. The assertions of probabilistic formulations are in form of safety levels. The simulation process of the corbels performed by the tools mentioned above is divided into several stages: model preparation in ATENA, randomization and final statistical assessment using FREET. The interaction between ATENA and FREET is managed by the software package SARA. SARA has been validated by many applications recently (Bergmeister, *et al.* 2002, Pukl, *et al.* 2003, 2003).

The stochastic models (described by probability density functions (PDF)) of the materials and geometries used for the corbels were taken from Spaethe (1992), Strauss, *et al.* (2003), and JCSS 2000. The stochastic models are related with each other by correlation coefficients collected in correlation matrices. Randomization of the corbel parameters, using the information of the stochastic models and the correlation matrices together with an advanced Monte Carlo Latin Hypercube Sampling (LHS) technique included in FREET, makes it possible to reduce the number of samples. This technique is essential for time-consuming nonlinear FE calculations. Additional information about the numerical techniques implemented within FREET is given by Novák, *et al.* (2003) and Voøechovský and Novák (2003). Finally, the outcomes as defined by the monitoring points of each of the samples are taken to the assessment part of the software FREET.

The assessment part contains statistical, reliability and sensitivity methods to evaluate resulting samples of selected response functions/limit state functions. These features serve for the validation of the corbel models and the corbels' safety level.

## 3. Analysis of the corbels

### *3.1. Experimental programs*

The corbels investigated in this study are taken from two experimental programs.

The first ones are derived from Kriz and Raths (1965). Their work was carried out in 1964 at the Research and Development Laboratories of the Portland Cement Association. A large number of

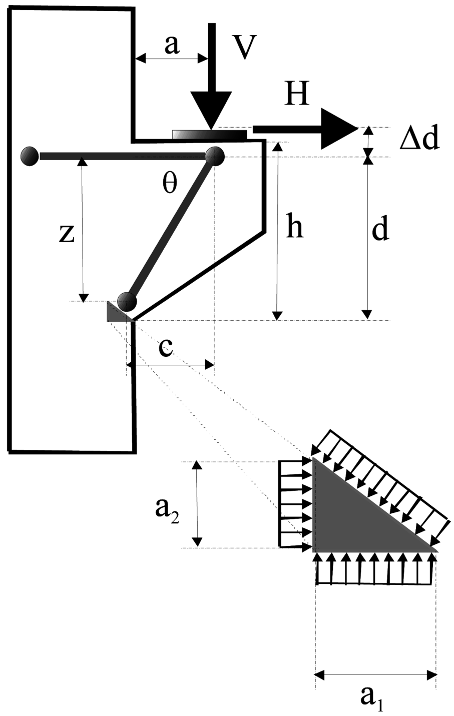


Fig. 1 Corbel sketch with strut-and-tie model

specimens was tested (124 corbels subjected to vertical load only and 71 corbels subjected to combined vertical and horizontal loads) in three stages: exploratory test, vertical load, vertical and horizontal loads. The final aim of the Kriz-Raths study was to develop design criteria for these structures. The exploratory tests were further carried out to define testing procedures and reinforce ment detailing; the other stages systematically investigated the effects of several variables on corbel behavior. In particular, the following factors were varied during the experimental program: reinforcement ratio, concrete strength, ratio of shear span to effective depth (*a/d*), amount and distribution of stirrup reinforcement, size and shape of corbel, and ratio of the vertical to the horizontal load. A corbel sketch with the main geometric properties is shown in Fig. 1.

The exploratory tests showed that corbel strength is not significantly affected by the load carrying capacity of the column, that the compressive reinforcement in the corbel and the longitudinal bars in the column have little influence on the ultimate load, that cross-bars welded to the main reinforcement ends can avoid bond failure, and that main reinforcements bent near the corbel outer edge can create a very weak zone. Therefore, in subsequent tests, the reinforcements were set in a manner that ensured significant results were obtained.

All the specimens were built on a 203×305 mm column with two corbels arranged symmetrically to make the testing procedures easier. Three cylinders were taken for each specimen to determine the concrete compressive strength. For convenience, all the corbels were tested in an upside-down position. In order to capture post-peak behavior, a displacement control method was applied.

The second experimental program focuses on SFRC corbels in order to increase the amount of data on this material applied to corbels (Fattuhi 1990). As before, the overall aim was to obtain

Table 1 Corbel properties

| Corbel | Geometry | | | | | Concrete | Steel | |
|---|---|---|---|---|---|---|---|---|
| | $a$ [mm] | $h$ [mm] | $b$ [mm] | $d$ [mm] | $a/h$ | $f_{cm}$ [MPa] | $f_{ym}$ [MPa] | $A_s$ [mm$^2$] |
| KR13 | 152 | 559 | 203 | 513 | 0,27 | 31,58 | 352 | 260 |
| KR14 | 152 | 660 | 203 | 615 | 0,23 | 31,3 | 352 | 260 |
| KR21 | 152 | 660 | 203 | 615 | 0,23 | 27,01 | 298 | 400 |
| KR55 | 254 | 559 | 203 | 513 | 0,45 | 27,65 | 312 | 396 |
| KR80 | 152 | 559 | 203 | 513 | 0,27 | 16,75 | 300 | 510 |
| KR91 | 121 | 457 | 203 | 406 | 0,26 | 27,99 | 322 | 1014 |
| KR100 | 152 | 457 | 203 | 406 | 0,26 | 44,33 | 328 | 1014 |
| F23fr | 110 | 149 | 153 | 123 | 0,74 | 38,3 | 452 | 226 |
| F25 | 110 | 149 | 154 | 123 | 0,74 | 30,7 | 452 | 226 |
| F34 | 135 | 148 | 154 | 123 | 0,91 | 32,0 | 452 | 339 |
| F35fr | 135 | 149 | 155 | 123 | 0,91 | 30,4 | 452 | 339 |
| F37fr | 135 | 149 | 154 | 122 | 0,91 | 32,2 | 452 | 339 |

general design criteria for these structures.

The tests were performed on 32 RC corbels subjected to a vertical load. The SFRC was used in 26 specimens as shear reinforcement in order to improve the strength and the ductility. During the experimental program, the following factors were varied: volume ratio of the fibers, main reinforcements, and ratio of shear span to effective depth (*a/d*).

The steel fibers were hooked with a diameter of 0.5 mm and a length of 30 mm. The steel has an average tensile strength of 1100 MPa. Six different volume ratios from 1.0% to 2.5% were used. Seven different main reinforcements were used, ranging from 101 mm$^2$ to 509 mm$^2$ in different diameter combinations, with an average yielding strength of 451, 454, 452 and 427 MPa for 8, 10, 12, and 18 mm bars respectively. The shear span-to-depth ratio varies in a range from 0.40 to 0.92. For all the corbels, the column was designed with a 150×150-mm cross section and was reinforced with four 12 mm longitudinal bars and four 6mm lateral ties. 20 mm plastic spacers were used to ensure a concrete cover for the main bars.

The concrete properties of the corbels are derived from cast cubes and cylinders taken during the casting process. The experimental tests were carried out in the same way as for the RC specimens, i.e., in an upside-down configuration. The planned load control testing failed in the early stages, because a displacement control testing procedure was used for all the remaining specimens. The corbel properties and their results are reported in Table 1. An “fr“ suffix in a corbel name indicates an SFRC specimen. The fiber ratios are $V$=2.00% for F23 and F37 and $V$=1.50% for F35.

### *3.2. General model parameters*

The Kriz-Raths experimental program not only contains specimens exclusively subjected to vertical loads, but also specimens subjected to both vertical and horizontal loads. The FE simulations consider only specimens subjected to vertical loads. Seven corbels from the Kriz-Raths program and five from the Fattuhi program are investigated. These corbels show different failure

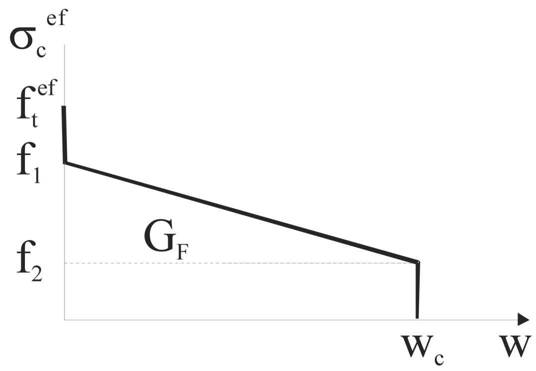


Fig. 2 Crack opening law for SFRC

modes and are evaluated at both deterministic and probabilistic levels.

In the 2D version of ATENA, the material was considered in a plane stress state, neglecting the real 3D behavior. The fixed smeared crack approach was used for the concrete model, including discrete reinforcement bars. In this way, modeling could be accomplished by combining standard elements, using a plain concrete model with rebar elements, based on a one-dimensional strain theory with a steel plasticity constitutive model.

The basic material concrete is modeled using the ATENA SBETA material with standard parameters (Cervenka 1985). Modeling the cracking effects by a smeared crack approach means that a real discrete crack is simulated by a band of localized strains. In the tensile field, pre-cracking behavior is assumed to be linear-elastic; after cracking, a fictitious crack band model based on a crack opening law and on fracture energy is used. As the crack strain is related to the element size, a softening law in terms of strain is written for each element; the crack opening law is preserved.

The crack opening law for SFRC is depicted in Fig. 2. $f_1$ is taken equal to the concrete tensile strength $f_t$ and $f_2$ is calculated according to ACI Committee 544 with the equation (ACI Committee 544);

$$f_2 = 0.772F\frac{L}{D}V_f \qquad (1)$$

where $F$ is a bond factor (ranging from 1 to 1.2), $L$ is the fiber length, $D$ is the fiber diameter and $V_f$ is the volume ratio of the fibers. Finally, the fracture energy $G_f$ is computed as the area under the curve.

In the ascending branch of the compressive field, the CEB-FIP Model Code 90 (CEB 1993) formulation is adopted, while post-peak behavior is assumed to be linearly descending. A different number provided as output denotes every region (tensile or compressive, pre- or post-peak) and can be used to evaluate concrete failure.

The failure criterion is based on experimental results of Kupfer, *et al.* (1969). It is divided in tensile failure and compressive failure zones: if the domain is reached in a tensile zone, a crack occurs. Using the current stress state, the corresponding value on the domain can be found and used to build the uniaxial stress-strain curve.

Concrete is modeled with a SBETA element, a reduced integration quadrilateral element in which the material law is evaluated only at centroid.

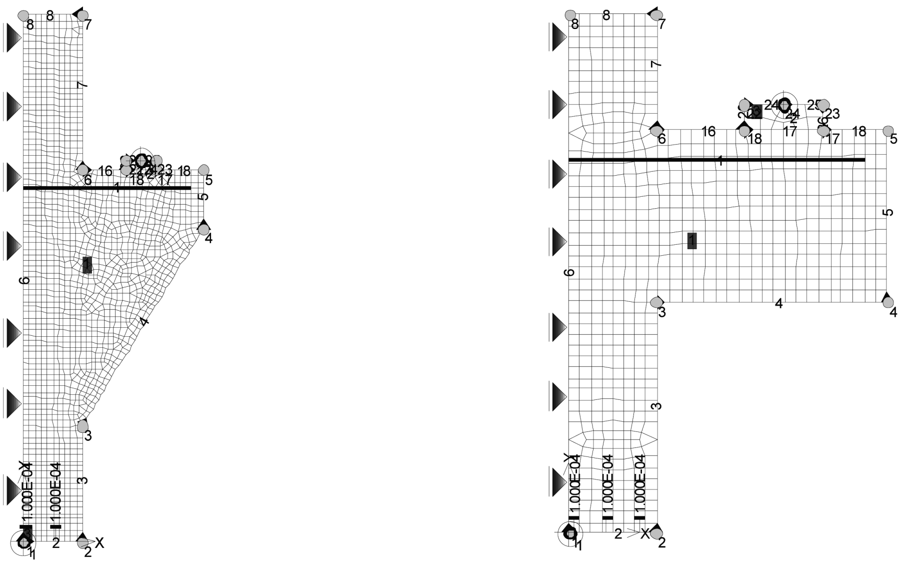


Fig. 3 FE discretization for Kriz-Raths (left) and Fattuhi (right) corbels

Reinforcing bars are inserted following the discrete approach. Truss elements are used with a bi-linearly elastic, perfectly plastic uniaxial constitutive model. Perfect connection with superposed concrete mesh is assumed, i.e., slip between steel and concrete is not accounted for.

An example of the FE discretization used in the numerical modeling is depicted in Fig. 3. The model contains about 1400 and 650 concrete elements for Kriz-Raths and Fattuhi corbels respectively and about 30 steel elements. All the corbels are vertically symmetrical not to have bending effects; therefore, the half-specimen can be modeled within ATENA in order to save computational time.

In the numerical investigations, a displacement control method is applied. In particular, a displacement is imposed at the column base while the bearing plate is constrained not to move in the vertical direction. Since the crack pattern and failure modes are strictly related, a comparison of the pictures taken during experiments with the numerical crack propagation is performed to check if the numerical simulation is able to capture the experimental failure mode.

### *3.3. Probabilistic model parameters*

The probabilistic simulation is accomplished by the software package SARA, which manages the interaction between ATENA and FREET.

The solution procedure is as follows:

- Modeling of the deterministic problem within ATENA. In this stage, the main hypotheses of structural behavior can be and should be verified.
- Randomization of the computational model considering material uncertainties. The randomization is based on LHS and suitable PDF distributions available in FREET.
- LHS allows the creation of manageable sample sets used for repeated ATENA analyses. In this study, 50 sample sets are used.

Table 2 Basic random variables (*SFRC)

| | variable | distribution | COV |
|---|---|---|---|
| Concrete | $E_c$ | Lognormal 2-par. | 0.08 |
| | $f_t$ | Lognormal 2-par. | 0.12 |
| | $f_c$ | Normal | 0.10 |
| | $G_f$ | Weibull min. 2-par. | 0.17 / 0.25* |
| Steel | $E_s$ | Normal | 0.03 |
| | $f_y$ | Normal | 0.05 |

Table 3 Correlation matrix

| | $E_c$ | $f_t$ | $f_c$ | $G_f$ | $E_s$ | $f_y$ |
|---|---|---|---|---|---|---|
| $E_c$ | 1 | 0.7 | 0.9 | 0.5 | 0 | 0 |
| $f_t$ | | 1 | 0.8 | 0.9 | 0 | 0 |
| $f_c$ | | | 1 | 0.6 | 0 | 0 |
| $G_f$ | | | | 1 | 0 | 0 |
| $E_s$ | | | | | 1 | 0 |
| $f_y$ | | | | | | 1 |

– Running the repeated analyses of the randomized problem within ATENA.
– Statistical assessment of the monitored sample sets obtained by ATENA within FREET – reliability index and sensitivity parameters are accessible.

The basic random variables chosen to investigate the corbels are: the elastic modulus $E_c$, the tensile strength $f_t$, the cylindrical compressive strength $f_c$ and the fracture energy $G_f$ of concrete, and the elastic modulus $E_s$ and the yielding strength $f_y$ of steel.

For these basic random variables, the stochastic models are summarized in Table 2.

In order to capture the statistical correlation between the individual basic variables, a correlation matrix based on intuitive judgement and experimental results (Bergmeister, *et al.* 2002) was used.

The statistical numerical outcomes serve for the evaluation of the structural behavior in general and provides insight into the reliability and sensitivity of the single components of the structure. Furthermore, the fitting of the statistical numerical outcomes by suitable PDF allows the exploration of the physical interaction of the structural components and delivers suitable PDFs for reliability considerations regarding the loading. This probabilistic approach can thus be customized to compare the safety level obtained by the calculations with the one suggested by design codes (CEN 1998).

### 3.4. Analysis of results

The first aim of the simulation was to test the FE code's capabilities to capture real structural behavior. Table 4 shows the results regarding the ultimate load. The failure modes are indicated as: T for reinforcement tie tensile failure, DS for diagonal splitting, CE for corbel end failure, C for compressive strut failure and S for shear failure. In the table, the experimental results are compared with ATENA and SARA calculations. The former is a single deterministic analysis, whereas the latter is a probabilistic evaluation based on the basic variables shown in Table 2. The mean value

Table 4 Corbel result comparison

| Corbel | Exp. failure | $V_{exp}$ [kN] | ATENA deterministic | | SARA probabilistic | |
|---|---|---|---|---|---|---|
| | | | $V$ [kN] | $(V_{num}-V_{exp})/V_{num}$ | $V_m \pm s$ [kN] | $(V_{num}-V_{exp})/V_{num}$ |
| KR13* | T | 266 | 279 | 4,9% | 287 ± 14 | 7,9% |
| KR14 | DS | 374 | 367 | -1,9% | 359 ± 13 | -4,0% |
| KR21 | DS | 423 | 405 | -4,3% | 411 ± 14 | -2,8% |
| KR55 | CE | 269 | 255 | -5,2% | 255 ± 10 | -5,2% |
| KR80 | C | 370 | 371 | 0,3% | 372 ± 13 | 0,5% |
| KR91 | S | 546 | 585 | 7,1% | 593 ± 29 | 8,6% |
| KR100 | S | 761 | 758 | -0,4% | 756 ± 31 | -0,7% |
| F23fr | T | 127 | 131 | 3,1% | 131 ± 3 | 3,1% |
| F25 | DS | 109 | 103 | -5,5% | 103 ± 4 | -5,5% |
| F34 | DS | 114 | 106 | -7,0% | 106 ± 5 | -7,0% |
| F35fr | S | 125 | 122 | -2,4% | 121 ± 3 | -3,2% |
| F37fr | T | 140 | 144 | 2,9% | 144 ± 6 | 2,9% |

*Corbel number 13 has a smaller experimental failure load because of a used steel with a yielding strength of 420 MPa.

Table 5 Results of SARA statistical simulation

| Corbel | Probabilistic Results | | | | | |
|---|---|---|---|---|---|---|
| | Distribution | Mean | Standard deviation | COV | Skewness | $V_5$ [kN] |
| KR13 | Lognormal 3-par. | 287 | 14 | 0,05 | -0,221 | 264 |
| KR14 | Normal | 359 | 13 | 0,04 | / | 337 |
| KR21 | Weibull max. 3-par. | 411 | 14 | 0,03 | -0,004 | 388 |
| KR55 | Weibull min. 2-par. | 255 | 10 | 0,04 | -0,961 | 236 |
| KR80 | Lognormal 3-par. | 372 | 13 | 0,03 | -0,413 | 350 |
| KR91 | Weibull min. 2-par. | 593 | 29 | 0,05 | -0,920 | 538 |
| KR100 | Weibull max. 3-par. | 756 | 31 | 0,04 | 0,116 | 706 |
| F23fr | Weibull max. 3-par. | 131 | 3 | 0,02 | 0,223 | 126 |
| F25 | Weibull max. 3-par. | 103 | 4 | 0,04 | 0,184 | 96 |
| F34 | Lognormal 3-par. | 106 | 5 | 0,05 | -0,023 | 97 |
| F35fr | Weibull max. 3-par. | 121 | 3 | 0,02 | -0,682 | 115 |
| F37fr | Weibull max. 3-par. | 144 | 6 | 0,04 | -0,410 | 134 |

$V_m$ and the standard deviation $s$ for the ultimate load are shown for each corbel.

The average difference of the ultimate load regarding the experimental values is 3.7% for the deterministic and 4.3% for the mean value obtained from the probabilistic calculation. It can be concluded that the agreement between the numerical and experimental program, for both normal and SFRC corbels, is excellent. Despite these excellent results, it should be borne in mind that the experimental results rely on only a small number of specimens. The numerical sample sets of 50 realizations and the stochastic models for concrete properties, taken from literature, Spaethe 1992,

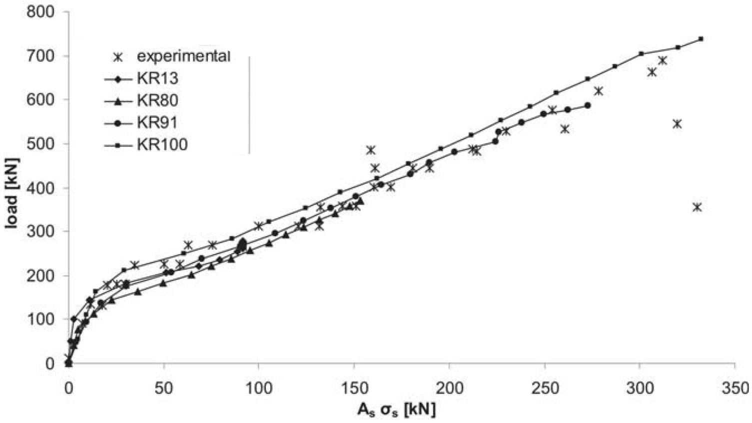


Fig. 4 Load vs. steelstress - numerical to experimental results - Kriz-Raths corbels

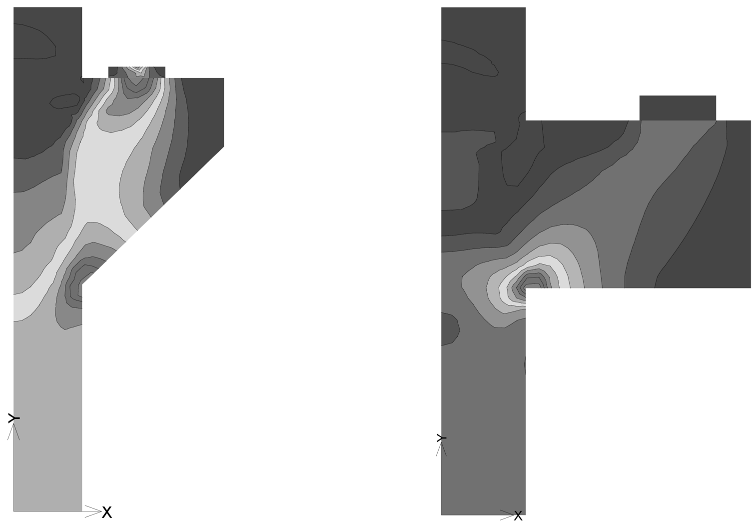

Fig. 5 Modelled compressive principal strain for Kriz-Raths (left) and Fattuhi (right) corbels

Strauss, *et al.* (relatively 2003), and JCSS 2000, lead to a variability of the ultimate load of *COV* = 0.02 - 0.09. This realtively small scattering and the coincidence of the numerical deterministic results with the experimental results confirm the adequacy of these approaches.

Table 5 shows the outcomes of the PDF fitting process at 50 realizations performed for each of the considered corbels. The Weibull max. 3-parameter function appeared to be the most suitable mathematical theoretical probability distribution for the resistance capacity. In the following, the 5% fractile $V_5$, also shown in Table 5, serves for the comparison with the Eurocode format.

Apart from the failure pattern and ultimate strength observations, model variables monitored during the loading were also of interest in order to understand the mechanical process taking place in the structure. Fig. 4 shows the steel force vs. the vertical load of the numerically extracted and the experimental data from Kriz-Raths corbels, *a/d* = 0.30. During the whole loading process, the numerical simulations coincide with the experiments, which indicates once more the ability of the chosen tools.

Fig. 5 shows the mechanical behavior of corbels for two different shapes. The minimum principal strain rendering clearly shows the compressed zones with the main strut and the singularity points in evidence. This demonstrates the power of the code for analyzing the concrete under complex

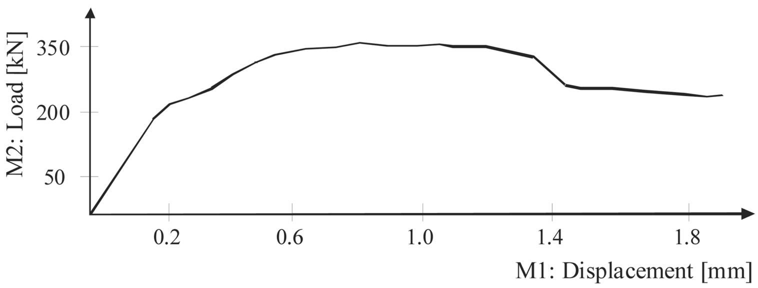


Fig. 6 Load-displacement curve for corbel KR14

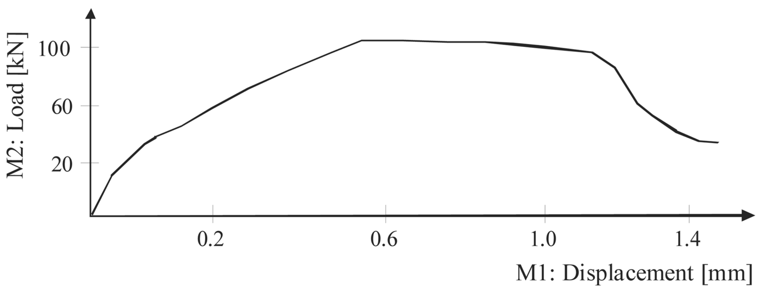


Fig. 7 Load-displacement curve for corbel F25

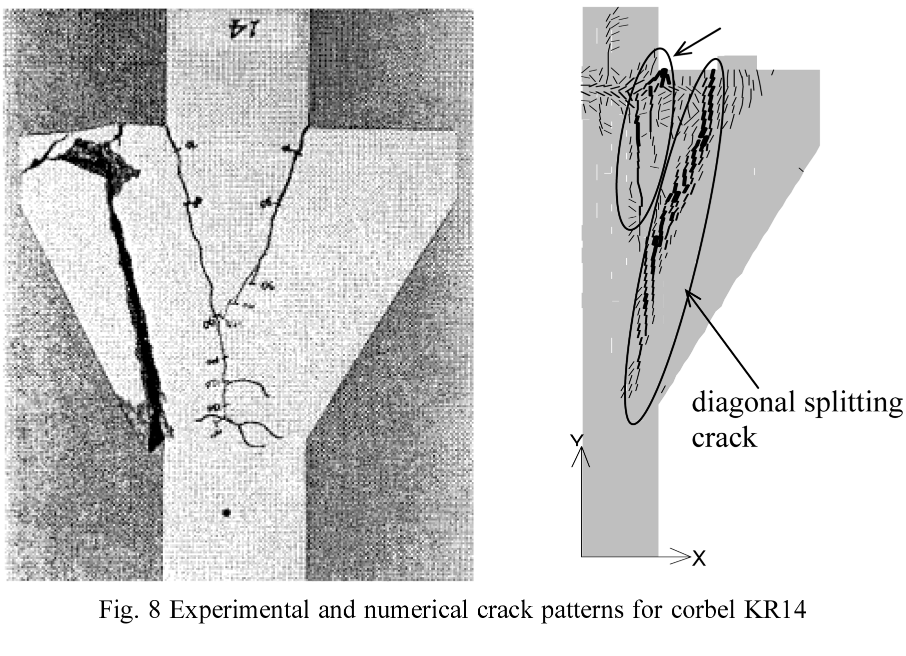


Fig. 8 Experimental and numerical crack patterns for corbel KR14

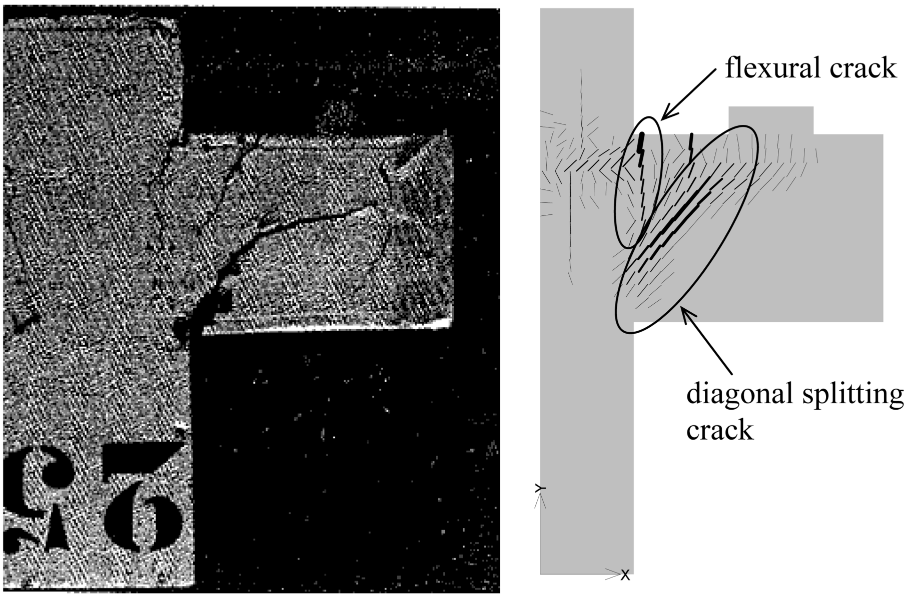


Fig. 9 Experimental and numerical crack patterns for corbel F25

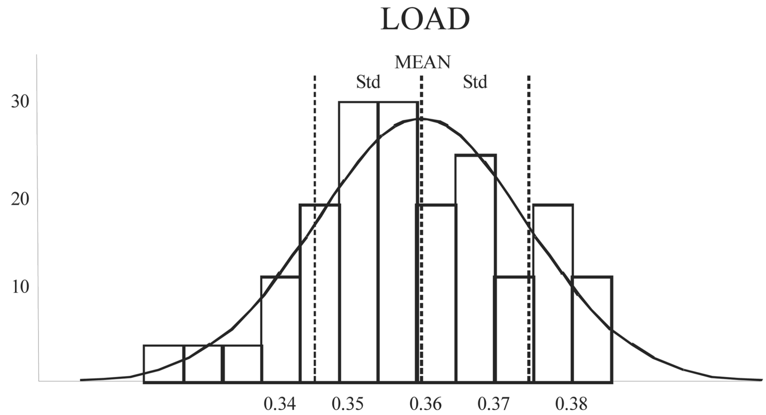


Fig. 10 Histogram and fited pdf (Normal) for corbel KR14

stress states. More detailed outcomes for two selected corbels are given in the next section.

### *3.5. Detailed outcomes for corbels KR14 and F25*

The calculated load displacement curves of the corbels under examination are shown in Fig. 6 and Fig. 7. The displacement is measured at the column bottom, whereas the load is measured at the bearing plate. The maximum load is 367 kN and 103 kN for corbels KR14 and F25 respectively, where the experimental ultimate loads are 374 kN and 109 kN. Furthermore, the curves explicitly predict the failure processes. In fact, the post-peak branch of the curve shows a significant ductile behavior due to the steel yielding followed by a compression-shear failure.

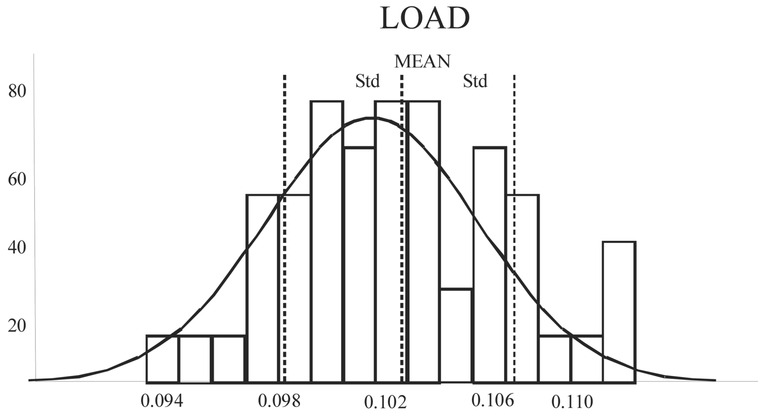


Fig. 11 Histogram and fited pdf (Weibull) for corbel F25.

Table 6 Sensitivity of structural response to variables

| | Variable | Ultimate load sensitivity | | Variable | Ultimate load sensitivity |
|---|---|---|---|---|---|
| Corbel KR14 | $f_y$ | 0.88 | Corbel F25 | $f_y$ | 0.88 |
| | $G_f$ | 0.32 | | $f_c$ | 0.36 |
| | $f_t$ | 0.27 | | $E_c$ | -0.34 |
| | $E_c$ | 0.15 | | $f_t$ | -0.24 |

Furthermore, the visible crack pattern was of interest. The calculated crack pattern, shown in Fig. 8 and Fig. 9, demonstrates that they are similar to the experimental ones. Both corbels are characterized by diagonal splitting failure, as can be clearly seen in the figures. At the first stage, the flexural crack patterns are fully developed. With increasing load, the compressed concrete fails by shear-compression and the diagonal splitting is revealed by a crack line extending from the bearing plate towards the end of the inclined bottom face of the corbel.

The probabilistic consideration of the ultimate limit state results in histograms is shown in Fig. 10 and Fig. 11. For instance, corbel KR14 has a mean value of 359 kN and a 5% fractile of 337 kN. Applying the curve fitting procedure to the ultimate load of the simulated samples then leads to a Weibull max. 3-parameter function as the most suitable PDF for the probability distribution. The

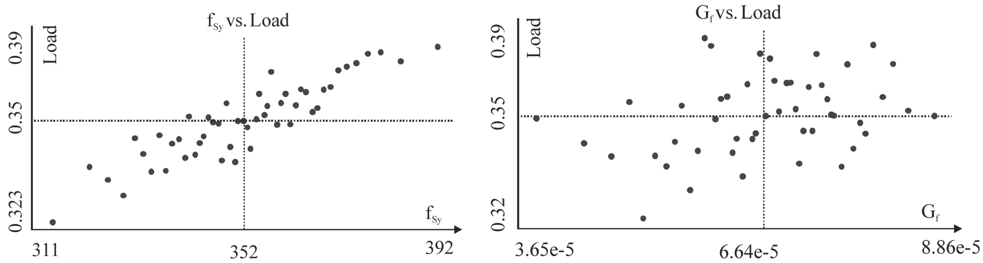


Fig. 12 Sensitivity plot for the first two variables of corbel KR14

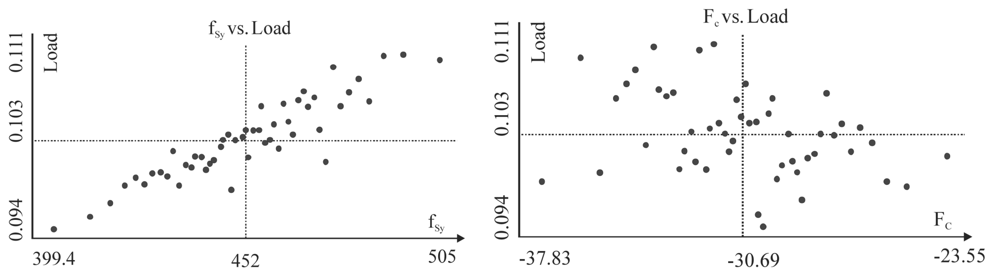


Fig. 13 Sensitivity plot for the first two dominant variables of corbel F25

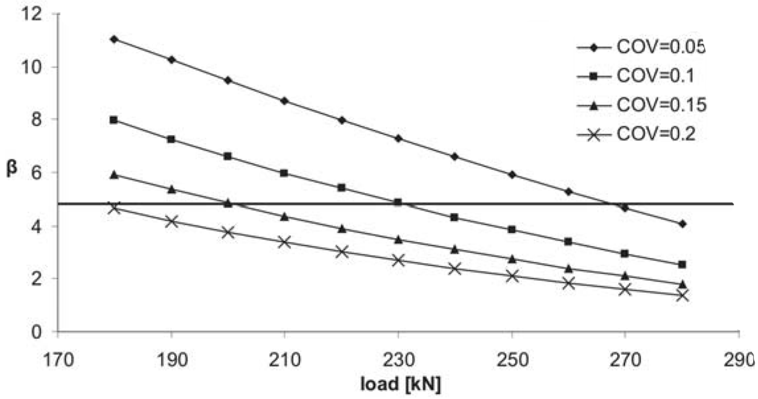


Fig. 14 Reliability assessment for the ultimate load of corbel KR14

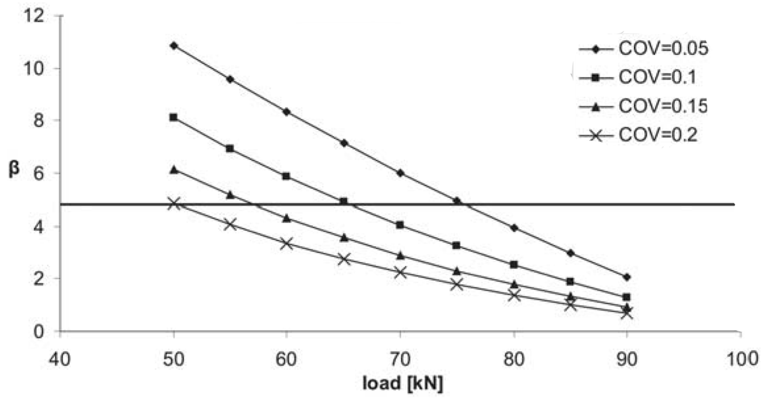


Fig. 15 Reliability assessment for the ultimate load of corbel F25

same examination applied to corbel F25 yields to a mean value of 103 kN, and to a 5% fractile of 96 kN. As a descriptive function, a Weibull max. 3-parameter function can be taken as a suitable distribution for the description of the numerical results.

When working with probabilistic approaches, the sensitivity parameters are important; they show parameter influence on results. The performed sensitivity study regarding the ultimate load of the corbels leads to the rank-order correlation coefficients as shown in Table 6. For both corbels, the numerical analysis shows that the steel yielding strength $f_y$ has the highest influence on the results, which is indicated by a high positive value of the correlation coefficient. $G_f$ and $f_t$ for corbel KR14 and $f_c$ and $E_c$ for corbel F25 are nearly equally influencing the ultimate load with a lower factor.

Fig. 12 and Fig. 13 show the virtually simulated correlation between load and the first two variables. For both of the corbels, the first variable $f_y$ has a very high positive correlation with respect to the load, whereas the second variables have a lower positive correlation.

A further step in the investigation of the corbels was the evaluation of the allowed load for a required safety index equal to 4.7 according to Eurocode (corresponding to a failure probability $p_f = 10^{-6}$). This study was performed with a variable mean value and four different coefficients of variations *COV* for the action.

Fig. 14 and Fig. 15 depict the results of this study for the two typical corbels KR14 and F25. As expected, the safety index $\beta$, a function of the mean value and the COV of the action, decreases with increasing action and increasing COV.

As can be seen from the illustration of corbel KR14, if the load is characterized by a high $COV$=0.2, only a load of about 180 kN can be accepted if the target limit of $\beta$=4.7 is to be satisfied. On the other hand, if it is possible to assure that the variability of the load is smaller than $COV$=0.05 (which is not probable as it is a strong requirement), a load of about 265 kN is allowed. For corbel F25 and a $COV$=0.2, only a load of about 50 kN can be accepted, whereas for a $COV$=0.05, a load of about 75 kN is allowed. These considerations are based on normal distributed density functions.

As a first approximation, these graphs are a fundamental basis for the design of corbels, since awareness of the statistical moments of the external loads for the demanded safety index $\beta$ (including scattering of the material, geometry and the load) can be the determining factor for the design.

## 4. Comparison with the Eurocode format

One can use the numerical outcomes presented above in combination with the Eurocode formulations to evaluate whether the probabilistic investigation can highlight some safety margins hidden by the general rules of the code.

The basis of the investigation is the design load calculated according to Eurocode 2 (CEN 1998) using a Strut-and-Tie model as depicted in Fig. 1. The design procedure includes an additional horizontal force $H$ = 0.2 $V$, which was applied according to the code.

Eq. (2) shows the constraints of the span-to-height ratio regarding the Eurocode:

$$0.4 \leq \frac{a}{h} \leq 1.0 \tag{2}$$

While some of the investigated corbels are out of this limit, they are calculated with the same procedure as a first approximation. The SFRC corbels are considered as general corbels.

To calculate the design values for the material properties, the following procedure was used. The characteristic value for steel and concrete strength can be calculated as:

$$f_{yk} = f_{ym} - 1.645 s_{steel} \quad \text{and} \quad f_{ck} = f_{cm} - 1.645 s_{concrete} \tag{3}$$

where $s$ is the standard deviation.

For the calculation of $s$, general mean values of the coefficient of variation $COV$ were applied:

$$COV_{steel} = \frac{s_{steel}}{f_{ym}} = 0.035 \quad \text{and} \quad COV_{concrete} = \frac{s_{concrete}}{f_{cm}} = 0.1 \tag{4}$$

Substituting Eq. (4) in Eq. (5) leads to:

$$f_{yk} = 0.94 f_{ym} \quad \text{and} \quad f_{ck} = 0.84 f_{cm} \tag{5}$$

While the characteristic to the design values are related by:

$$f_{sd} = \frac{f_{yk}}{1.15} \quad \text{and} \quad f_{cd} = \frac{f_{ck}}{1.5} \tag{6}$$

Therefore, the design values can be calculated starting from the mean values as reported in Table 1 by:

$$f_{sd} = 0.82 f_{ym} \quad \text{and} \quad f_{cd} = 0.56 f_{cm} \tag{7}$$

The angle between the strut and the tie (Fig. 1) for the Eurocode model was computed by:

$$tg\theta = \frac{z}{c} = \frac{d - 0.5a_2}{a + 0.5a_1} \tag{8}$$

where

$$a_1 = \frac{V}{0.6\alpha f_{cd} b} \quad \text{and} \quad a_2 = d - \sqrt{d^2 - 2a_1 c} \tag{9}$$

Table 7 Comparison of the safety index from nonlinear numerical results vs Eurocode format

| Corbel | $V_{EC2,\ steel}$ [kN] | $V_{EC2,\ concrete}$ [kN] | $V_{EC2}$ [kN] | $V_5$ [kN] | $\gamma = \frac{V_5}{V_{EC2}}$ | Failure |
|---|---|---|---|---|---|---|
| KR13 | 125 | 352 | 125 | 264 | 2,11 | steel |
| KR14 | 139 | 389 | 139 | 337 | 2,42 | steel |
| KR21 | 170 | 336 | 170 | 388 | 2,28 | steel |
| KR55 | 122 | 335 | 122 | 236 | 1,93 | steel |
| KR80 | 169 | 187 | 169 | 350 | 2,07 | steel |
| KR91 | 308 | 248 | 248 | 538 | 2,17 | concrete |
| KR100 | 359 | 392 | 359 | 706 | 1,97 | steel |
| F23fr | 50 | 53 | 50 | 126 | 2,54 | steel |
| F25 | 51 | 58 | 51 | 96 | 1,87 | steel |
| F34 | 58 | 54 | 54 | 97 | 1,80 | concrete |
| F35fr | 57 | 52 | 52 | 115 | 2,21 | concrete |
| F37fr | 59 | 55 | 55 | 134 | 2,44 | concrete |

and $b$ is the corbel depth.

Solving the Strut-and-Tie structure, the force in the steel $F_s$ has to be less than or equal to the design steel ultimate load:

$$F_s = \frac{1}{z}(H(z+\Delta d)+vc) \leq F_{sd} = f_{sd}A_s \tag{10}$$

The verification of the concrete has to be carried out according to shear design rules:

$$V \leq V_{Rd2} = 0.6\alpha f_{cd} bz \sin\theta \cos\theta \tag{11}$$

These formulations are performed on the different corbels to get the design load, see Table 7. Furthermore, the safety factor $\gamma$ between the numerically calculated 5% fractile and the design load according to Eurocode are reported in this table. The values are compared with those proposed by Eurocode, namely 1.15 for steel failure and 1.50 (variable loads) for concrete failure.

In summary, the calculated safety factor is always greater than the one proposed by the Eurocode. In fact, if the 5% fractile of the numerical ultimate load $V_5$ is compared with the design value of the Eurocode, the required safety index, ($\gamma$= 1.15 for steel), is by far satisfied. Considering the smallest safety margin of this study ($\Delta\gamma$= 1.87–1.15 = 0.72), the nonlinear numerical investigation allows a more accurate description of material behavior and more efficient design within the requirements of the safety margins.

## 5. Three-dimensional analyses

Up to now, all effects have been considered using two dimensional computational models. It was of general interest whether 3D effects emphasize or lower the properties of the corbels. Therefore, a 3D deterministic analysis has been performed for some of the corbels already investigated in 2D. The 3D investigations also have been performed with ATENA.

### *5.1. Structural modeling*

Similary to the 2D version, there are also several different material models available in ATENA 3D. Most of them are based on a fracture-plasticity approach which combines constitutive models for tensile (fracturing) and compressive (plastic) behavior.

The fracture model is based on the classical orthotropic smeared crack formulation and crack band model. It employs the Rankine failure criterion and exponential softening, and it can be used as rotated or fixed crack model. For the problem at hand, the fixed crack approach is used. The crack opening is computed from the total value of fracturing strain plus the current increment of fracturing strain, and this sum is multiplied by the characteristic length, which is calculated as a size of the element projected into the crack direction.

The hardening/softening plasticity model is based on Menétrey-Willam (1995) failure surface using a return mapping algorithm for the integration of constitutive equations. New stress state in the plastic model is computed using a predictor-corrector formulation, where the plastic corrector is computed directly from the yield function by the return mapping algorithm.

Special attention is given to the combination of fracture and plasticity models. The combined algorithm is based on a recursive substitution and makes it possible to formulate the two models

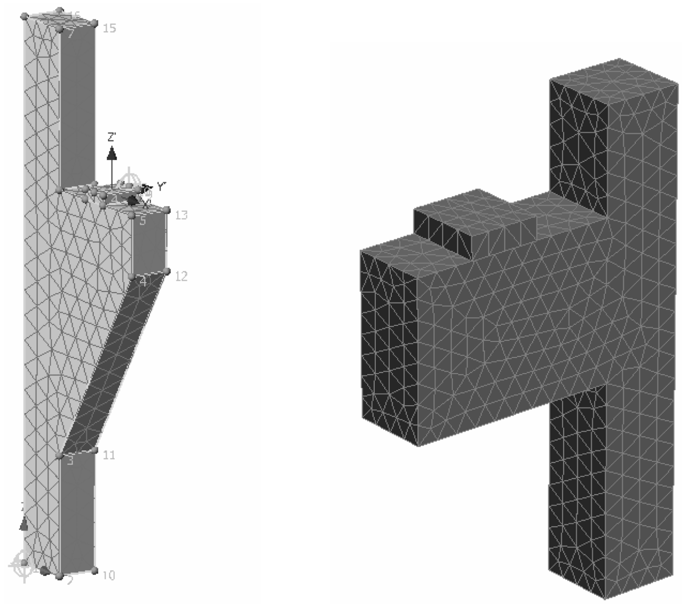


Fig. 16 3D FE discretization for Kriz-Raths (left) and Fattuhi (right) corbels

separately. However, both models are developed within the framework of the return mapping algorithm, which guarantees a solution for all magnitudes of strain increment.

ATENA allows the user to define the evolution law for some selected parameters, such as elastic modulus, tensile and compressive strength, shear retention factor for the fixed crack approach, and reduction of tensile strength due to lateral compressive stress. Furthermore, the tension stiffening can be simulated by specifying a suitable factor: in the tension softening diagram, the tensile stress cannot drop below a tension stiffening factor multiplied by the tensile strength.

The reinforcements are modeled by using the same formulation already described for the 2D version of the code.

The FE meshes used for the 3D analyses are shown in Fig. 16. The ATENA solid element library

Table 8 3D deterministic results

| Corbel | Exp. failure | $V_{exp}$ [kN] | Deterministic | | Deterministic | |
|---|---|---|---|---|---|---|
| | | | $V_{ATENA\ 2D}$ [kN] | Difference | $V_{ATENA\ 3D}$ [kN] | Difference |
| KR14 | DS | 374 | 367 | -1,9% | 384 | 2,7% |
| KR21 | DS | 423 | 405 | -4,3% | 448 | 5,9% |
| KR55 | CE | 269 | 255 | -5,2% | 272 | 1,1% |
| F23fr | T | 127 | 131 | 3,1% | 142 | 11,8% |
| F25 | DS | 109 | 103 | -5,5% | 115 | 5,5% |
| F34 | DS | 114 | 106 | -7,0% | 129 | 13,2% |

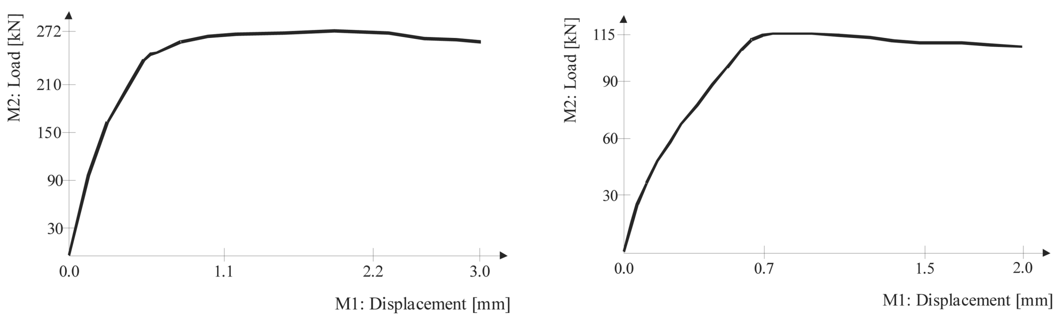


Fig. 17 Load-displacement curve for corbel KR55 (left) and F25 (right)

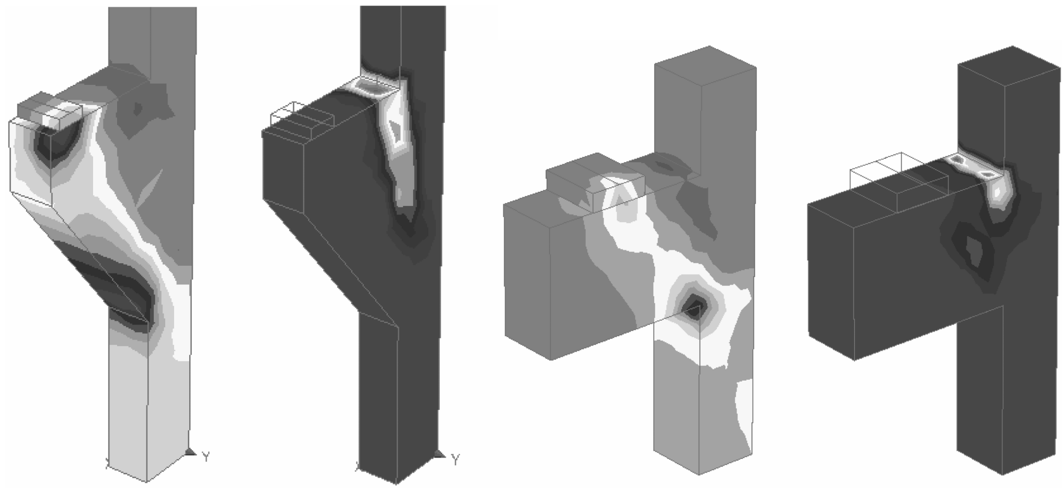

Fig. 18 Min. principal strain and crack width for KR55 (left) and for F25 (right)

includes tetrahedral elements, brick elements and wedge elements, all using linear isoparametric formulation. Here, tetrahedral elements are used with different sizes depending on the corbel. In fact, a fine mesh is more suitable for Fattuhi corbels (6146 elements) whereas Kriz-Raths corbels require a less refined mesh (1552 elements).

Due to double symmetry, only a quarter of the specimen was modeled.

### 5.2. Results of the 3D modeling

The essential numerical results of the 3D analyses are reported in Table 8. The numerical simulations provide very good results for the Kriz-Raths corbels, whereas there are deviations for the Fattuhi specimens.

In general, the ultimate loads of these 3D considerations are higher than the 2D calculations. Since the steel reinforcements are modelled as in the 2D analyses, it could be hypothesized that the difference in the ultimate loads is due to the alternative constitutive model used for the 3D concrete elments. Considering the mesh of the Fattuhi specimens in more detail it could be recognised that the 2D mesh size is about half size of the 3D mesh. This and the circumstance that tetrahedrons are lower order elements then bricks results to the conclusion that a finer mesh would overcome the deteceted deviations. Therefore using a finer mesh for the Fattuhi specimens will lead to fully compareable results calculated by the 2D models.

In Fig. 17, the load displacement curves for the investigated corbels are reported. Both the specimens exhibit a ductile behavior with a long plastic plateau after steel yielding. The load displacement curve for corbel F25 can be compared with the analogous 2D outcome: the shape of the curve is similar and the ultimate load is achieved nearly for the same displacement.

Finally, in Fig. 18, some further outcomes from ATENA 3D are shown. In particular, the compressive strut can be located in the corbel by the minimum principal strain. Moreover, it is possible to evaluate the crack pattern based on the crack width and, thereby, to assess the failure mode.

## 6. Conclusions

The major objective of this research program was to test the capability of nonlinear calculation techniques for capturing the real behavior of structures. For this purpose, both deterministic and probabilistic finite element analyses of reinforced concrete corbels were compared with experimental testing programs.

Deterministic analysis was based on two and three-dimensional models of nonlinear finite element codes. These analyses provide not only information about the ultimate load, but also more information about structural behavior, such as the failure mode, the crack pattern, and the stress-strain distribution in the reinforcement and concrete materials.

The 2D analysis coincides perfectly with the experimental outcomes, not only for the ultimate load, but also for the whole fracture process (deviations are smaller than 4%). This indicates the adequacy of sophisticated nonlinear techniques to perform quasi-experimental tests in a numerical format.

The outcomes of the 3D analysis are higher for some of the tested models than the experimental and 2D results. With high probability, these deviations are caused by coarse meshes or low order elements of the 3D FEM models. The fracture energy $G_f$ could not be determined by the experimental program, but it could be detected that it has a dominant influence on the 3D elements. It was demonstrated in the 3D considerations by the missing descending ductile behavior after the ultimate load.

In the second part of the research program, probabilistic analysis takes the center stage. Our research demonstrates that the scattering of the ultimate load for this kind of structures, using ordinary concrete properties, is between 5% and 9%. For the investigated corbels, the most sensitive factors are yield strength, fracture energy, and compressive strength. The low scattering value is due to the dominance of the yield strength parameters. The curve fitting process shows that the resistance of the corbels can be described very well by a Weibull function (*COV* 0.05).

Based on these outcomes, a comparison with the Eurocode format was possible. The analyses have demonstrated that the simple Strut-and-Tie model proposed by the Eurocode is sufficient to obtain safe results for design. The hidden safety margin, evaluated on the basis of the safety factors, is at minimum 60% ($\Delta\gamma$= 1.87–1.15 = 0.72 … 1.15 *1.62 = 1.87).

The main outcomes of our research are as follows: nonlinear probabilistic calculation, especially the advanced technique used in this contribution, can be used for more efficient corbel design within the allowed safety margins. Especially for prefabricated corbel, probabilistic analysis can serve as a basis for optimized structural design and reduced costs accordingly. Furthermore, probability-based sensitivity studies can be applied in practically oriented design in order to detect the most dominating variables that need to be carefully controlled.

## References

ACI Committee 544 (1988), "Design considerations for steel fiber reinforced concrete (ACI 544.4R-88)", *Manual of Concrete Practice, Part 5*, American Concrete Institute, Detroit, MI, 563-590.

Ali, M. A. and White, R. N. (2001), "Consideration of compression stress bulging and strut degradation in truss modeling of ductile and brittle corbels", *Eng. Struct.,* **23**(3), March, 240-249.

Bergmeister, K., Strauss, A., Eichinger, E. M., Kolleger, J., Novak, D., Pukl, R., Cervenka, V. (2002), "Structural analysis and safety assessment of existing concrete structures", *The First Fib Congress*, Osaka, Japan.

CEB, (1993). Comité Euro-International du Béton, *CEB – FIP Model Code 90*, Bulletin d'Information No. 213/214, 1993.

CEN (1998), EN1992 Eurocode 2: Design of concrete structures.

Cervenka, J, Cervenka, V., Eligehausen, R. (1998), "Fracture-plastic material model for concrete, application to analysis of powder actuated anchors", *Proc. FRAMCOS 3,* 1107-1116.

Cervenka, V. (1985), "Constitutive model for cracked reinforced concrete", *J. ACI, Proc.* **82,** Nov-Dec., No. 6, 877-882.

Cervenka, V. (2000), "Simulating a response" *Conc. Eng. Int.*, **4**(4), 45-49.

Cervenka, V. (2002), "Computer simulation of failure of concrete structures for practice", *The First Fib Congress*, Osaka, Japan, Session 13, 289-304.

Crisfield, M.A. (1983), "An arc-length method including line search and accelerations", *Int. J. Num. Meth. in Eng.*, **19**, 1269-1289.

Fattuhi, N.I. (1990), "Strength of SFRC corbels subjected to vertical load", *J. Struct. Eng.* ASCE, **116**(3).

Holnicki-Szulc, J. and Gierlinski, J. T. (1997), "Structural analysis, design and control by the Virtual Distortion Method", *Eng. Struct.,* **19**(4), April 1997, 335-336.

JCSS (2000), *Probabilistic Model Code*, 12th Draft, Joint Committee of Structural Safety.

Kriz, L. B. and Raths, C. H. (1965), "Connections in precast concrete structures – strength of corbels", *PCI J.*, **10**(1), February 1965.

Kupfer, H., Hilsdorf, H. K., Rusch, H., (1969), "Behavior of concrete under biaxial stresses", *ACI J., Proceedings*, **66**(8), Aug, 656-666.

Menétrey, P. and Willam, K. J. (1995). "Triaxial failure criterion for concrete and its generalization", *ACI Struct. J.*, **92**(3), May-June 311-317.

Mordini, A. and Strauss, A. (2005), "Deterministic and probabilistic finite element analysis of reinforced concrete corbels", *Internal Report of Institute of Structural Engineering,* University of Natural Resources and Applied Life Sciences, Vienna, March 2005.

Novak, D., Vorechovsky, M., Rusina, R. (2003), "Small-sample probabilistic assessment – software FREET", *ICASP 9, 9th International Conference on Applications of Statistics and Probability in Civil Engineering*, San Francisco, USA, July 6-9, 91-96.

Pukl, R., Cervenka, V., Strauss, A., Bergmeister, K., Novak, D. (2003), "An advanced engineering software for probabilistic-based assessment of concrete structures using nonlinear fracture mechanics", *Applications of Statistics and Probability in Civil Engineering*, Der Kiureghian, Madanat & Pestana (eds.), Millpress, Rotterdam.

Pukl, R., Novak, D., Bergmeister, K. (2003), "Reliability assessment of concrete structures", *Computational Modeling of Concrete Structures: Euro-C 2003*, March 17-20, 2003, St. Johann im Pongau, Austria, 817-825.

Spaethe, G. (1992), *Die Sicherheit Tragender Baukonstruktionen*, Springer-Verlag, Wien, New York.

Strauss, A., Bergmeister, K., Santa, U., Pukl, R., Cervenka, V., Novák, D. (2003), "Non destructive reliability analysis of concrete structures numerical concepts and material models for existing concrete structures", *Deutsche Gesellschaft für Zerstörungsfreie Prüfung: International Symposium (NDT-CE 2003) Non-Destructive Testing in Civil Engineering 2003*, Berlin, September 16-19, 2003.

Vorechovsky, M. and Novak, D. (2003), "Statistical correlation in stratified sampling", *ICASP 9, 9th International Conference on Applications of Statistics and Probability in Civil Engineering*, San Francisco, USA, July 6-9, 119-124.

*CC*